Z. angew. Math. Phys. 52 (2001) 254–288
0044-2275/01/020254-35 $ 1.50+0.20/0

Zeitschrift für angewandte Mathematik und Physik ZAMP

A spatially nonlocal model for polymer-penetrant diffusion

David A. Edwards

Abstract. Diffusion of a penetrant in a polymer entanglement network cannot be described by Fick's Law alone; rather, one must incorporate other nonlocal effects. In contrast to previous viscoelastic models which have modeled these effects through hereditary integrals in time, a new model is presented exploiting the disparate lengths of the polymer in the glassy (dry) and rubbery (saturated) states. This model leads to a partial integrodifferential equation which is nonlocal in space. The system is recast as a moving boundary-value problem between sets of coupled partial differential equations. Using singular perturbation techniques, sorption in a semi-infinite polymer is studied on several time scales with varying exposed interface conditions. Though some of the results match with those from viscoelastic models, new physically relevant behaviors also appear. These include the formation of stopping fronts and overshoot in the pseudostress.

Mathematics Subject Classification (2000). 35B25, 35C15, 35C20, 35K60, 35R35, 73B18, 76R99, 80A22.

Keywords. Spatial nonlocality, moving boundary-value problems, non-Fickian diffusion, polymer-penetrant systems, singular perturbation methods, asymptotics.

1. Introduction

The nearly "designer" properties of polymers have made them a preferred material in many industries. For instance, polymers are routinely used in conjunction with various penetrants or diluents in gaseous or liquid form. One unusual, yet industrially exploitable, feature of such polymer-penetrant systems is a change of state in the polymer from a *rubbery* state when it is nearly saturated to a *glassy* state when it is nearly dry. The change in material properties associated with the change of state can then be utilized in various manufacturing processes.

These polymer-penetrant systems often exhibit anomalous behavior, such as "Case II diffusion," where a sharp change-of-state interface moves with constant speed [1]. Such phemomena cannot be explained by simple Fickian diffusion, which postulates that the chemical potential $\tilde{\mu}$ of the system is a function of the penetrant concentration $\tilde{C}$ only. Though all the physical mechanisms responsible for these phenomena are not known, most scientists agree that one important factor is a nonlocal dependence of the dynamics upon the configuration of the polymer

entanglement network. In many polymer-penetrant systems, these nonlocal effects are as important to the transport process as the well-understood Fickian dynamics [2].

Though nonlocal effects are considered responsible for much of the unusual behavior seen in polymer-penetrant systems, the overwhelming majority of studies have considered memory effects: that is, those that are nonlocal in time only (for instance, see [3]–[5]). These effects have been modeled by assuming that $\tilde{\mu}$ depends not only on $\tilde{C}$, but also on an osmotically-induced viscoelastic "swelling pressure" [6], which is related to the trace of the stress tensor in the polymer entanglement network [6]–[9].

However, these nonlocal effects in *time* can be thought of as resulting partly from the disparate *length* scales in polymer-penetrant systems. Consider a penetrant molecule diffusing through an entangled polymer network. Polymers form very long chains which can be orders of magnitude larger than the penetrant molecules. Thus, the entanglement network can be heuristically visualized as a mass of tangled spaghetti-like strands. In the glassy state, the network can be highly ordered or even crystalline [10]. After the rubber transition, the network becomes more and more disordered.

Thus, one can see that the entanglement network forms a series of interconnected "pockets" through which the penetrant must diffuse [11]. These pockets can open or close through the formation of "holes" by even a limited oscillation of one or two polymer strands [10], [12]. This "pocket" model holds even when the polymer molecules are more rigid and rodlike [13], and the idea of the entanglement network restricting free diffusion is also the centerpiece of the reptation model of polymer-polymer diffusion [11], [13].

Since links between polymer chains form on these pockets, the dynamics will depend not only on local properties, but also on properties within a neighborhood of characteristic length β^{-1}, which we shall call the *dependence length*. In fact, it is well known that the stress in the system is dependent on the configuration of the polymer strands [13], [14]. Therefore, it is important to examine the possibility that some of the nonlocal effects are spatial in nature. This type of nonlocal spatial modeling also appears in some stochastic models of this type of behavior [15].

There are several ways that one can construct a characteristic dependence length. One way is to relate β to the relaxation time of the stress in the viscoelastic model using the molecular diffusion coefficient $\tilde{D}$. Due to this simplistic relationship, we also expect the new model to capture the polymer-penetrant dynamics well. Another is to let β^{-1} be the length of the polymer chain. However, since the molecule is quite often folded and twisted in some disordered configuration, it is better to interpret β^{-1} as the radius of the smallest sphere that contains the polymer chain.

Clearly β depends on the strength of the entanglement of the polymer network, which is directly related to the amount of penetrant $\tilde{C}$ [11]. At first blush, it might seem appropriate to use the standard diffusion equation to describe the

system while allowing $\tilde{D}$ to vary in some nonlocal spatial way upon $\tilde{C}$. This is because increasing $\tilde{C}$ allows the polymer network to disentangle, and increased mobility of the polymer chains increases $\tilde{D}$ as more "holes" form [10]. However, these sort of models were originally used (with nonlocal effects in time) to explain Case II diffusion in polymers [14], [16]–[18], and they ultimately proved unsuccessful. Therefore, we adapt the previous model by assuming that $\tilde{\mu}$ depends on a "pseudostress" $\tilde{\sigma}$ which has nonlocal spatial dependence. (The choice of terminology will be apparent later.) Though proposing a model of this type to study polymer-penetrant systems is rather unusual, certainly the key ideas have appeared in other disciplines. For instance, spatial nonlocalities have been used successfully for many years to model biological systems [19]–[21].

The formation of the model leads to a partial integrodifferential equation, which can be restated as a system of two coupled partial differential equations. By making physically appropriate assumptions, the system is reduced to a moving boundary-value problem, where different operators hold on either side of the glass-rubber interface. We solve the problem of sorption into a semi-infinite medium on two different time scales and for two different types of conditions.

If the permeability of the exposed surface is high, on the shorter time scale the front moves in a purely Fickian way, even though the solution in the rubbery region does not obey a Fickian operator. For lower permeabilities, the front initially moves in a linear fashion, then as $\tilde{t} \to \infty$, asymptoting to a $\sqrt{\tilde{t}}$ behavior with a backward shift. Again, this is similar to Fickian systems with a radiation boundary condition [22].

On the longer time scale, the front will actually stop as $\tilde{t} \to \infty$. This represents an equilibrium between the diffusive forces trying to move the front along and the pseudostress, which acts to retard front motion [23]. This stopping front behavior has not been seen in models for these systems which involve only memory effects.

2. Governing equations

In order to incorporate the nonlocal spatial effects of polymer entanglement networks into our model, we postulate that the chemical potential $\tilde{\mu}$ is a function of $\tilde{C}$ and $\tilde{\sigma}$, where $\tilde{\sigma}$ is described by the following (in one dimension):

$$\tilde{\sigma} = -\frac{1}{2}\int_{-\infty}^{\infty} f\left(\tilde{C}(\tilde{x}',\tilde{t}), \frac{\partial \tilde{C}}{\partial \tilde{x}}(\tilde{x}',\tilde{t})\right) \exp\left[-\left|\int_{\tilde{x}'}^{\tilde{x}} \beta(\tilde{C}(z,\tilde{t}))\,dz\right|\right] d\tilde{x}'. \tag{2.1}$$

As defined in (2.1), $\tilde{\sigma}$ solves the evolution equation

$$\frac{\partial}{\partial \tilde{x}}\left[\frac{1}{\beta(\tilde{C})}\frac{\partial \tilde{\sigma}}{\partial \tilde{x}}\right] - \beta(\tilde{C})\tilde{\sigma} = f\left(\tilde{C}(\tilde{x},\tilde{t}), \frac{\partial \tilde{C}}{\partial \tilde{x}}(\tilde{x},\tilde{t})\right). \tag{2.2}$$

In particular, we call $\tilde{\sigma}$ the *pseudostress* since, though a nonstate variable, its behavior matches closely that of the stress in the polymer network in the viscoelastic

models [24]. We also note that (2.2) is quite similar to the evolution equation in [5] with $\partial/\partial\tilde{t}$ replaced by $\partial^2/\partial\tilde{x}^2$—in other words, we replace one part of the diffusion operator with another. This relationship, along with the fact that we may construct a β by combining the relaxation time with the diffusion coefficient, provides strong evidence that this model should produce many results that agree with the models that are nonlocal in time.

The next step is to determine the proper form for f. Following the discussion in [5], [25], and [26] for memory effects, we use a form which is linear in both $\tilde{C}$ and $\partial\tilde{C}/\partial\tilde{x}$, namely

$$f\left(\tilde{C}(\tilde{x},\tilde{t}),\frac{\partial\tilde{C}}{\partial\tilde{x}}(\tilde{x},\tilde{t})\right)=-\eta\tilde{C}(\tilde{x},\tilde{t})+\nu\frac{\partial\tilde{C}}{\partial\tilde{x}}(\tilde{x},\tilde{t}). \tag{2.3}$$

where η and ν are positive constants. Some discussion of (2.3) is appropriate. Substituting (2.3) into (2.2), we obtain the following evolution equation for $\tilde{\sigma}$:

$$\frac{\partial}{\partial\tilde{x}}\left[\frac{1}{\beta(\tilde{C})}\frac{\partial\tilde{\sigma}}{\partial\tilde{x}}\right]-\beta(\tilde{C})\tilde{\sigma}=-\eta\tilde{C}(\tilde{x},\tilde{t})+\nu\frac{\partial\tilde{C}}{\partial\tilde{x}}(\tilde{x},\tilde{t}). \tag{2.4}$$

As we approach the far field (and hence can neglect the $\tilde{x}$-derivative terms), we see that a positive value for $\tilde{C}$ implies a positive value for $\tilde{\sigma}$. Since we wish to think of $\tilde{\sigma}$ as analogous to a stress, this makes sense. Similarly, we note that if we have a positive concentration flux at a point $\tilde{x}$, then $\partial\tilde{C}/\partial\tilde{x}$ is negative there. We would expect a positive flux to increase the stress, and hence the signs match here as well.

The evolution equation (2.4) for $\tilde{\sigma}$ coupled to the standard conservation of mass equation $\partial\tilde{C}/\partial\tilde{t}=-\partial\tilde{J}/\partial\tilde{x}$, provide the system which we must solve. Since

$$\tilde{J}=-K(\tilde{C})\frac{\partial\tilde{\mu}(\tilde{C},\tilde{\sigma})}{\partial\tilde{x}}=-\left[\tilde{D}(\tilde{C})\frac{\partial\tilde{C}}{\partial\tilde{x}}+E(\tilde{C})\frac{\partial\tilde{\sigma}}{\partial\tilde{x}}\right], \tag{2.5}$$

where $K(\tilde{C})$ is some nonlinear function and $E(\tilde{C})$ is a function of proportionality, the conservation of mass equation becomes

$$\frac{\partial\tilde{C}}{\partial\tilde{t}}=\frac{\partial}{\partial\tilde{x}}\left[\tilde{D}(\tilde{C})\frac{\partial\tilde{C}}{\partial\tilde{x}}+E\frac{\partial\tilde{\sigma}}{\partial\tilde{x}}\right], \tag{2.6}$$

where in (2.6) we have assumed that $E(\tilde{C})$ is constant, as in [5], [7].

The polymer entanglement network exists in one of two states. In the glassy state when the polymer is nearly dry, the polymer chains are well-ordered and severely entangled. In contrast, in the rubbery state when the polymer is nearly saturated, the network disentangles and the characteristic length of a chain grows

[10], [11]. Thus $\beta(\tilde{C})$ changes greatly as the polymer goes from the glassy state to the rubbery state. However, the differences in $\beta(\tilde{C})$ *within* phases are qualitatively negligible when compared with the differences *between* phases. Hence, we model $\beta(\tilde{C})$ by its average in each phase, yielding the following functional form:

$$\beta(\tilde{C}) = \begin{cases} \beta_{\mathrm{g}}, & 0 \le \tilde{C} \le \tilde{C}_* \text{ (glass)} \\ \beta_{\mathrm{r}}, & \tilde{C}_* < \tilde{C} \le \tilde{C}_{\mathrm{c}} \text{ (rubber)}, \end{cases} \tag{2.7}$$

where $\tilde{C}_*$ is the concentration at which the rubber-glass transition occurs and $\tilde{C}_{\mathrm{c}}$ is a saturation level for the polymer.

We use a canonical example for systems of this type. We wish to model the sorption of an initially dry semi-infinite polymer, so we have that

$$\tilde{C}(\tilde{x}, 0) = 0. \tag{2.8}$$

Due to the form of the evolution equation (2.4), we must impose a boundary condition on the pseudostress at the exposed edge $\tilde{x} = 0$. At the present time, we leave it arbitrary:

$$\tilde{\sigma}(0, \tilde{t}) = \tilde{\sigma}_{\mathrm{b}}(\tilde{t}). \tag{2.9}$$

At the exposed edge, we also apply a *radiation condition*, which indicates that the flux through the inside of the film is proportional to the difference between the concentration at the edge of the film and the exterior concentration $\tilde{C}_{\mathrm{ext}}$:

$$-\left[\tilde{D}(\tilde{C})\frac{\partial \tilde{C}}{\partial \tilde{x}} + E\frac{\partial \tilde{\sigma}}{\partial \tilde{x}}\right](0, \tilde{t}) = \tilde{k}[\tilde{C}_{\mathrm{ext}} - \tilde{C}(0, \tilde{t})]. \tag{2.10}$$

Note that (2.10) implies that the flux desorbed depends directly on the concentration at the boundary. Therefore, in sorption problems with low permeability, we expect the concentration at the boundary to grow slowly, approaching $\tilde{C}_{\mathrm{ext}}$ as $\tilde{t} \to \infty$.

Our problem will involve matching the solutions of the two equations where $\beta = \beta_{\mathrm{g}}$ and $\beta = \beta_{\mathrm{r}}$. Thus, it is necessary to impose conditions at the moving boundary $\tilde{s}(\tilde{t})$ between the two regions. In the region where the polymer is rubbery, we will use a superscript "r" on the dependent variables; in the region where the polymer is glasssy, we will use a superscript "g". We begin by assuming continuity of concentration at the specified transition value $\tilde{C}_*$:

$$\tilde{C}^{\mathrm{r}}\left(\tilde{s}(\tilde{t}), \tilde{t}\right) = \tilde{C}_* = \tilde{C}^{\mathrm{g}}\left(\tilde{s}(\tilde{t}), \tilde{t}\right). \tag{2.11}$$

In addition, we assume that there is a fundamental change that takes place in the polymer as we go from glass to rubber. Experimentally, this has been shown to be related to a stretching of the polymer. The penetrant used up by the polymer in this stretching is directly analogous to the energy used up in melting in a standard

two-phase heat conduction problem. Hence, we follow the same sort of derivation [5], [22] to obtain the standard condition that the difference between the flux in and the flux out is proportional to the speed of the front, *i.e.*,

$$[\tilde{J}]_{\tilde{s}} = -\tilde{a}\frac{d\tilde{s}}{d\tilde{t}},$$

where $\tilde{a}$ is a constant and where we have defined the operator $[f]_{\tilde{s}} \equiv f^{\mathrm{g}}(\tilde{s}^{+}(\tilde{t}),\tilde{t}) - f^{\mathrm{r}}(\tilde{s}^{-}(\tilde{t}),\tilde{t})$. (Note that this definition includes continuity of flux as a special case.) Substituting our expression for $\tilde{J}$ from (2.10) into the above, we have the following:

$$\left[\tilde{D}\frac{\partial \tilde{C}}{\partial \tilde{x}} + E\frac{\partial \tilde{\sigma}}{\partial \tilde{x}}\right]_{\tilde{s}} = \tilde{a}\frac{d\tilde{s}}{d\tilde{t}}. \tag{2.12}$$

Due to the nature of the operator in the time-dependent models, one needed to impose only continuity of pseudostress there, with the value undetermined [27]. However, since the evolution equation (2.4) for pseudostress is second order, we either need two conditions (one in $\tilde{\sigma}$ and one in $\partial\tilde{\sigma}/\partial\tilde{x}$) or a specified value for $\tilde{\sigma}$. Since the "Stefan condition" (2.12) is already a condition on $\partial\tilde{\sigma}/\partial\tilde{x}$, we must impose continuity of pseudostress at a predetermined value $\tilde{\sigma}_*$:

$$\tilde{\sigma}^{\mathrm{r}}\left(\tilde{s}(\tilde{t}),\tilde{t}\right) = \tilde{\sigma}_* = \tilde{\sigma}^{\mathrm{g}}\left(\tilde{s}(\tilde{t}),\tilde{t}\right). \tag{2.13}$$

We assume that $\tilde{\sigma}_* > 0$ in a sorption experiment.

In order to restate the problem in dimensionless variables, we let

$$x = \tilde{x}\beta_{\mathrm{c}}, \quad t = \nu E\beta_{\mathrm{c}}^2\tilde{t}, \quad s(t) = \beta_{\mathrm{c}}\tilde{s}(\tilde{t}), \quad C(x,t) = \frac{\tilde{C}(\tilde{x},\tilde{t})}{\tilde{C}_{\mathrm{c}}}, \quad \sigma(x,t) = \frac{\tilde{\sigma}(\tilde{x},\tilde{t})}{\nu\tilde{C}_{\mathrm{c}}},$$

$$\sigma_* = \frac{\tilde{\sigma}_*}{\nu\tilde{C}_{\mathrm{c}}}, \qquad \sigma_{\mathrm{b}}(t) = \frac{\tilde{\sigma}_{\mathrm{b}}(\tilde{t})}{\nu\tilde{C}_{\mathrm{c}}}, \qquad C_* = \frac{\tilde{C}_*}{\tilde{C}_{\mathrm{c}}}, \qquad a = \frac{\tilde{a}}{\tilde{C}_{\mathrm{c}}}, \qquad k = \frac{\tilde{k}}{\nu E\beta_{\mathrm{c}}},$$

$$D(C) = \frac{\tilde{D}(\tilde{C})}{\nu E}, \qquad C_{\mathrm{ext}} = \frac{\tilde{C}_{\mathrm{ext}}}{\tilde{C}_{\mathrm{c}}},$$

where $\tilde{C}_{\mathrm{c}}$ and β_{c} are arbitrary for now. Then equations (2.6), (2.4), (2.8)–(2.11), (2.13), and (2.12) reduce to

$$\frac{\partial C}{\partial t} = \frac{\partial}{\partial x}\left[D(C)\frac{\partial C}{\partial x} + \frac{\partial \sigma}{\partial x}\right], \tag{2.14}$$

$$\frac{\partial}{\partial x}\left[\frac{\beta_{\mathrm{c}}}{\beta(C)}\frac{\partial \sigma}{\partial x}\right] - \frac{\beta(C)}{\beta_{\mathrm{c}}}\sigma = -\frac{\eta}{\nu\beta_{\mathrm{c}}}C + \frac{\partial C}{\partial x}, \tag{2.15}$$

$$C(x,0) = 0, \tag{2.16a}$$

$$\sigma(0,t) = \sigma_{\mathrm{b}}(t), \tag{2.16b}$$

$$D(C)\frac{\partial C}{\partial x}(0,t) + \frac{\partial \sigma}{\partial x}(0,t) = k[C(0,t) - C_{\mathrm{ext}}], \tag{2.17}$$

$$C^{\mathrm{r}}\left(s(t),t\right) = C_* = C^{\mathrm{g}}\left(s(t),t\right), \tag{2.18}$$

$$\sigma^{\mathrm{r}}\left(s(t),t\right) = \sigma_* = \sigma^{\mathrm{g}}\left(s(t),t\right), \tag{2.19}$$

$$\left[D(C)\frac{\partial C}{\partial x} + \frac{\partial \sigma}{\partial x}\right]_s = a\dot{s}, \tag{2.20}$$

where the dot indicates differentiation with respect to t. These are the equations which we will be using in our nonlinear analysis. A remark about (2.20) is appropriate. In other nonlocal models [5], it is possible to use the evolution equation for σ to rewrite the analogous front condition in terms of C only. Unfortunately, due to the second-order operator in (2.15), (2.20) cannot be simplified further.

In order to make the problem analytically tractable, we make one more simplifying assumption. As stated before, the diffusion coefficient often, though not always, increases dramatically as the polymer goes from the glassy to rubbery state [28]. However, changes *within* phases are less important. Hence, we perform the same averaging as we did with the relaxation time to obtain the following form for $D(C)$:

$$D(C) = \begin{cases} D_{\mathrm{g}}, & 0 \le C \le C_*, \\ D_{\mathrm{r}}, & C > C_*. \end{cases} \tag{2.21}$$

This piecewise-constant form for $D(C)$ has been used by Crank [14] to study these anomalous systems. More discussion of various physically appropriate forms for $D(C)$ and $E(C)$ can be found in Cohen and White [25].

Due to the forms of (2.7) and (2.21), we may treat $\beta(C)$ and $D(C)$ as constants. Thus we may combine equations (2.14) and (2.15) to obtain

$$\frac{\partial^3 C}{\partial x^2 \partial t} = D(C)\frac{\partial^4 C}{\partial x^4} - \frac{\eta\beta(C)}{\nu\beta_{\mathrm{c}}^2}\frac{\partial^2 C}{\partial x^2} + \frac{\beta(C)}{\beta_{\mathrm{c}}}\frac{\partial^3 C}{\partial x^3} + \frac{\beta^2(C)}{\beta_{\mathrm{c}}^2}\frac{\partial C}{\partial t} - \frac{\beta^2(C)D(C)}{\beta_{\mathrm{c}}^2}\frac{\partial^2 C}{\partial x^2}. \tag{2.22}$$

It can be shown that this operator also holds for σ.

In order to use a perturbation method, we must have a small parameter. Since the length of a swelled polymer chain (or the radius of a circumscribed sphere) is much larger than for a glassy polymer chain, we take $\beta_{\mathrm{r}}/\beta_{\mathrm{g}} = \epsilon$. (Note this is true because we are taking the ratio of the *reciprocal* of the length scales.)

3. Fickian fronts

Next we must specify the choice of the length scale β_c^{-1}. To begin, we use the geometric mean of our two characteristic length scales, β_g^{-1} and β_r^{-1}; hence $\beta_c = \sqrt{\beta_g \beta_r}$. Making this substitution into (2.15) and (2.22) yields

$$\frac{\partial^2 \sigma}{\partial x^2} - \frac{\beta^2(C)}{\beta_r \beta_g}\sigma = -\frac{\eta \beta(C)}{\nu \beta_r \beta_g} C + \frac{\beta(C)}{\sqrt{\beta_g \beta_r}} \frac{\partial C}{\partial x}, \tag{3.1}$$

$$\frac{\partial^3 C}{\partial x^2 \partial t} = D(C)\frac{\partial^4 C}{\partial x^4} - \frac{\eta \beta(C)}{\nu \beta_g \beta_r}\frac{\partial^2 C}{\partial x^2} + \frac{\beta(C)}{\sqrt{\beta_g \beta_r}}\frac{\partial^3 C}{\partial x^3} + \frac{\beta^2(C)}{\beta_g \beta_r}\frac{\partial C}{\partial t} - \frac{\beta^2(C) D(C)}{\beta_g \beta_r}\frac{\partial^2 C}{\partial x^2}. \tag{3.2}$$

Diffusion in the rubbery region is much more pronounced than in the glassy region, so we take $D_r = D_0 \epsilon^{-1}$. Making this substitution into (2.14), (3.1), and (3.2), we have the following equations in the rubbery region:

$$\frac{\partial C^r}{\partial t} = D_0 \epsilon^{-1}\frac{\partial^2 C^r}{\partial x^2} + \frac{\partial^2 \sigma^r}{\partial x^2}, \qquad 0 < x < s(t), \tag{3.3a}$$

$$\frac{\partial^2 \sigma^r}{\partial x^2} - \epsilon \sigma^r = -\epsilon \gamma C^r + \epsilon^{1/2}\frac{\partial C^r}{\partial x}, \qquad \gamma = \frac{\eta}{\nu \beta_r}, \tag{3.3b}$$

$$\frac{\partial^3 C^r}{\partial x^2 \partial t} = D_0 \epsilon^{-1}\frac{\partial^4 C^r}{\partial x^4} - \epsilon\gamma\frac{\partial^2 C^r}{\partial x^2} + \epsilon^{1/2}\frac{\partial^3 C^r}{\partial x^3} + \epsilon\frac{\partial C^r}{\partial t} - D_0\frac{\partial^2 C^r}{\partial x^2}, \tag{3.4}$$

while in the glassy region we obtain

$$\frac{\partial C^g}{\partial t} = D_g\frac{\partial^2 C^g}{\partial x^2} + \frac{\partial^2 \sigma^g}{\partial x^2}, \qquad x > s(t), \tag{3.5a}$$

$$\frac{\partial^2 \sigma^g}{\partial x^2} - \epsilon^{-1}\sigma^g = -\gamma C^g + \epsilon^{-1/2}\frac{\partial C^g}{\partial x}, \tag{3.5b}$$

$$\frac{\partial^3 C^g}{\partial x^2 \partial t} = D_g\frac{\partial^4 C^g}{\partial x^4} - \gamma\frac{\partial^2 C^g}{\partial x^2} + \epsilon^{-1/2}\frac{\partial^3 C^g}{\partial x^3} + \epsilon^{-1}\frac{\partial C^g}{\partial t} - D_g\epsilon^{-1}\frac{\partial^2 C^g}{\partial x^2}. \tag{3.6}$$

We note that with such a large diffusion coefficient in the rubbery region, we would expect the front to move in an $O(1)$ fashion only if a was correspondingly large. Therefore, we let $a = a_0\epsilon^{-1}$ in (2.20), yielding

$$\left(D_g\frac{\partial C^g}{\partial x} + \frac{\partial \sigma^g}{\partial x}\right)(s(t),t) - \left(D_0\epsilon^{-1}\frac{\partial C^r}{\partial x} + \frac{\partial \sigma^r}{\partial x}\right)(s(t),t) = a_0\epsilon^{-1}\dot{s}. \tag{3.7}$$

As a simplest possible test case, we consider the case where $k > O(\epsilon^{-1})$, in which case the leading order of (2.17) becomes $C^r(0,t) = C_{ext}$, where we have used the fact that $D(C)$ never becomes larger than $O(\epsilon^{-1})$. We have also assumed that

$C_{\text{ext}} \geq C_*$ in order to obtain a change of state. In this case, $\tilde{C}_{\text{ext}}$ is the natural choice for the characteristic penetrant concentration (since we do not expect the polymer to saturate at a higher level). Hence $C_{\text{ext}} = 1$ and we have

$$C^{\text{r}}(0,t) = 1. \tag{3.8}$$

Thus the polymer is always in the rubbery region when $x = 0$, so

$$s(0) = 0. \tag{3.9}$$

3.1. The rubbery region

First we consider the rubbery region. We assume a perturbation series in ϵ for our solutions:

$$C^{\text{r}}(x,t;\epsilon) = C_0^{\text{r}}(x,t) + o(1), \qquad \sigma^{\text{r}}(x,t;\epsilon) = \sigma_0^{\text{r}}(x,t) + o(1). \tag{3.10}$$

Substituting (3.10) into (3.3a), (2.18), and (3.8), we obtain, to leading order,

$$D_0 \frac{\partial^2 C_0^{\text{r}}}{\partial x^2} = 0, \qquad C_0^{\text{r}}\left(s(t),t\right) = C_*, \tag{3.11}$$

$$C_0^{\text{r}}(0,t) = 1. \tag{3.12}$$

Solving (3.11) subject to (3.12) yields the following:

$$C_0^{\text{r}}(x,t) = 1 - \frac{(1-C_*)x}{s}. \tag{3.13}$$

Substituting (3.10) into (3.3b), (2.16b), and (2.19), we have

$$\frac{\partial^2 \sigma_0^{\text{r}}}{\partial x^2} = 0, \qquad \sigma_0^{\text{r}}(0,t) = \sigma_{\text{b}}(t), \qquad \sigma_0^{\text{r}}\left(s(t),t\right) = \sigma_*, \tag{3.14}$$

the solution of which is

$$\sigma_0^{\text{r}}(x,t) = \sigma_{\text{b}}(t) - \frac{[\sigma_{\text{b}}(t) - C_*]x}{s}. \tag{3.15}$$

3.2. Glassy pseudostress and front position

In the glassy region, we assume a perturbation series in ϵ for our solutions:

$$C^{\mathrm{g}}(x,t;\epsilon) = C_0^{\mathrm{g}}(x,t) + o(1), \qquad \sigma^{\mathrm{g}}(x,t;\epsilon) = \sigma_0^{\mathrm{g}}(x,t) + o(1). \tag{3.16}$$

Substituting these series into (3.5b), we obtain $\sigma_0^{\mathrm{g}} = 0$ to leading order, which clearly does not satisfy the leading order of (2.19):

$$\sigma_0^{\mathrm{g}}\left(s(t),t\right) = \sigma_*. \tag{3.17}$$

Thus, an interior layer must be introduced in the pseudostress near the front.

Substituting (3.16) and our expression for σ_0^{g} into (3.5a) and (2.18), we obtain, to leading order,

$$\frac{\partial C_0^{\mathrm{g}}}{\partial t} = D_{\mathrm{g}} \frac{\partial^2 C_0^{\mathrm{g}}}{\partial x^2}, \tag{3.18}$$

$$C_0^{\mathrm{g}}\left(s(t),t\right) = C_*. \tag{3.19}$$

From the diffusive form of (3.18), it is reasonable to assume that there would not need to be an interior layer in the concentration, since the front condition (3.19) can be solved without one. Indeed this is the case, as can be shown.

Therefore, the only interior layer needed is in the pseudostress. Letting

$$\zeta = \frac{x - s(t)}{\epsilon^{1/2}}, \qquad \sigma^{\mathrm{g}}(x,t) = \sigma^{+}(\zeta,t) + o(1), \tag{3.20}$$

in (3.5b), (3.17), and the matching condition that $\sigma_0^{\mathrm{g}} \equiv 0$, we have

$$\frac{\partial^2 \sigma^{+}}{\partial \zeta^2} - \sigma^{+} = 0, \qquad \sigma^{+}(0,t) = \sigma_*, \qquad \sigma^{+}(\infty,t) = 0, \tag{3.21}$$

the solution of which is

$$\sigma^{+}(\zeta,t) = \sigma_* e^{-\zeta}. \tag{3.22}$$

Substituting our scalings in (3.20) into (3.7), we obtain, to leading order,

$$D_0 \frac{(1 - C_*)}{s} = a_0 \dot{s}, \tag{3.23}$$

where we have used (3.13). Continuing to simplify, we have

$$s(t) = 2b\sqrt{D_{\mathrm{g}} t}, \qquad b = \sqrt{\frac{D_0(1 - C_*)}{2a_0 D_{\mathrm{g}}}}, \tag{3.24}$$

where we have used (3.9) and assumed that $a_0 > 0$.

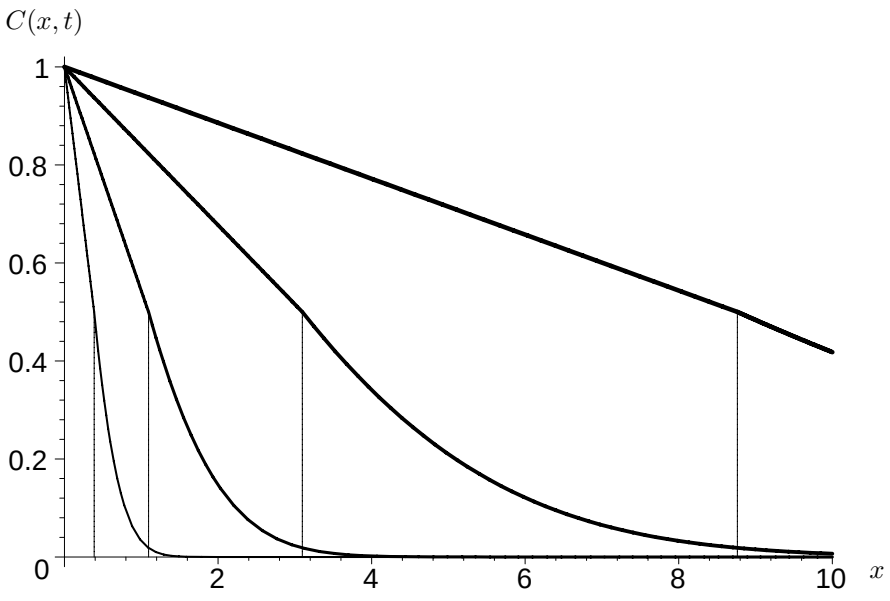

Figure 3.1.
In increasing order of thickness: $C(x,t)$ *vs.* x for $t = 0.1$, 0.8, 6.4, 5.12 and the parameters in (3.27a).

3.3. The glassy region: concentration

Substituting our series in (3.16) into (2.16a) yields the following:

$$C_0^{\mathrm{g}}(x,0) = 0. \tag{3.25}$$

Solving (3.18) subject to (3.19), (3.24), and (3.25), we have

$$C_0^{\mathrm{g}}(x,t) = C_* \frac{\operatorname{erfc}(x/2\sqrt{D_g t})}{\operatorname{erfc} b}. \tag{3.26}$$

Figure 3.1 shows a graph of the concentration *vs.* x for various times, as listed in the figure caption. The position of the front at each time is marked by a vertical line from $C = 0$ to $C = C_*$. The parameters chosen are listed below:

$$a_0 = 2, \qquad C_* = \frac{1}{2}, \qquad D_0 = 3, \qquad D_{\mathrm{g}} = 1. \tag{3.27a}$$

Note that as expected, we see standard Fickian-like behavior in the glassy region. In the rubbery region, the nonlocal behavior in space has the effect of enhancing the diffusion, and thus we obtain steady-state Fickian profiles.

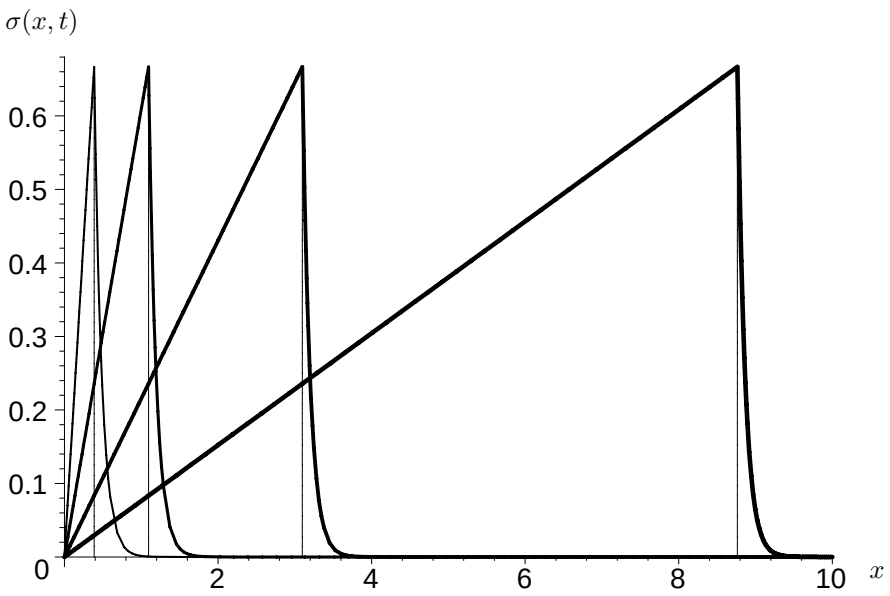

Figure 3.2.
In increasing order of thickness: $\sigma(x,t)$ *vs.* x for $t = 0.1$, 0.8, 6.4, 5.12 and the parameters in (3.27).

Figure 3.2 shows a graph of the pseudostress *vs.* x for the same times as in Fig. 3.1. The position of the front at each time is marked by a vertical line from $\sigma = 0$ to $\sigma = \sigma_*$. The figure uses the parameters in (3.27a) as well as the following additional ones:

$$\epsilon = 0.01, \qquad \sigma_{\rm b}(t) = 0, \qquad \sigma_* = \frac{2}{3}. \tag{3.27b}$$

Note that from the unstressed state, the pseudostress increases greatly in a narrow band about $x = s(t)$. This is due to the fact that there is a nonzero pseudostress in the rubbery region caused by the finite spatial memory there. In contrast, there is no pseudostress in the glassy region because of the inifinitesimal spatial memory there. These two regions must be matched together in a smooth diffusive way, which forces the creation of an interior layer.

4. Lower permeability

Now we examine the case where the permeability is not quite so large. We assume that $k = k_0\epsilon^{-1}$, and again normalize so that $C_{\rm ext} = 1$. Substituting this form into

(2.17), we obtain

$$D(C)\frac{\partial C}{\partial x}(0,t)+\frac{\partial \sigma}{\partial x}(0,t)=k_0\epsilon^{-1}[C(0,t)-1]. \tag{4.1}$$

If the polymer starts out in the glassy region, there is no balance because $D(C)=O(1)$ and $C(0,t)=1$ corresponds to the rubbery region. Therefore, the polymer at the exposed surface must always be rubbery and (4.1) becomes

$$D_0\frac{\partial C_0^{\mathrm{r}}}{\partial x}(0,t)=k_0[C_0^{\mathrm{r}}(0,t)-1], \tag{4.2}$$

where we have used the series in (3.10). Equation (4.2) now replaces (3.12) in our work from that section. The solution to (3.11) and (4.2) is given by

$$C_0^{\mathrm{r}}(x,t)=C_*+\frac{k_0 s(1-C_*)}{k_0 s+D_0}\left(1-\frac{x}{s}\right). \tag{4.3}$$

Note that in the limit that $k_0\to\infty$, (4.3) reduces to (3.13).

The new boundary condition does not affect our calculation of the pseudostress in either the glassy or rubbery regions. However, with (4.3) replacing (3.13) and letting

$$S(t)=s(t)+\frac{D_0}{k_0}, \tag{4.4}$$

(3.23) becomes

$$D_0\frac{(1-C_*)}{S}=a_0\dot{S},$$

the solution of which is

$$S(t)=\sqrt{2\frac{D_0(1-C_*)t}{a_0}+\frac{D_0^2}{k_0^2}}, \tag{4.5a}$$

$$s(t)=-\frac{D_0}{k_0}+\sqrt{2\frac{D_0(1-C_*)t}{a_0}+\frac{D_0^2}{k_0^2}}. \tag{4.5b}$$

Note that in the limit that $k_0\to\infty$, (4.5b) reduces to (3.24).

Since $s(t)$ is no longer proportional just to $t^{1/2}$, we cannot use similarity variables to obtain a solution. Therefore, we employ an integral method developed by Boley [29] for simpler diffusion problems and used extensively on systems with memory effects by Edwards [7], [24], [30]. We assume that the equations for the glassy region hold for the *entire* semi-infinite region for some function $T(x,t)$. Therefore, we have that

$$T(x,t)=C_0^{\mathrm{g}}(x,t), \qquad x>s(t). \tag{4.6}$$

This fictitious function T must satisfy the operator in (3.18) subject to the boundary data (3.19) and (3.25) and a *fictitious* boundary condition (FBC)

$$T(0,t) = f_{\rm b}(t). \tag{4.7}$$

Thus, we have

$$\frac{\partial T}{\partial t} = D_{\rm g}\frac{\partial^2 T}{\partial x^2}, \qquad T(x,0) = 0, \tag{4.8}$$

$$T(s(t),t) = C_*. \tag{4.9}$$

Using Laplace transforms, the solution of (4.8) subject to (4.7) can easily be shown to be

$$T(x,t) = \frac{x}{2\sqrt{\pi D_{\rm g}}}\int_0^t \frac{f_{\rm b}(z)}{(t-z)^{3/2}}\exp\left[-\frac{x^2}{4D_{\rm g}(t-z)}\right]dz. \tag{4.10}$$

Substituting (4.10) into (4.9), we obtain

$$\frac{s}{2\sqrt{\pi D_{\rm g}}}\int_0^t \frac{f_{\rm b}(z)}{(t-z)^{3/2}}\exp\left[-\frac{s^2}{4D_{\rm g}(t-z)}\right]dz = C_*. \tag{4.11}$$

Note that by using Boley's method we have reduced the problem to an integral equation in the unknowns s and $f_{\rm b}$.

4.1. Small-time asymptotics

We begin by looking at the solution for small time. Expanding (4.5b) for small time, we have

$$s(t) \sim \frac{k_0(1-C_*)t}{a_0}. \tag{4.12}$$

We note that since the concentration at the surface is not high as that in the previous section, the front moves more slowly, and in a manner proportional to the permeability. In order to obtain a solution for $C_0^{\rm g}$ that satisfies (4.11) at the front position given by (4.12), we must assume a form for $f_{\rm b}(t)$ that approaches a nonzero constant as $t \to 0$. Doing so, we obtain the following:

$$C_0^{\rm g} \sim C_* \operatorname{erfc}\left(\frac{x}{2\sqrt{D_g t}}\right), \quad t \to 0. \tag{4.13}$$

Figure 4.1 shows a graph of the concentration *vs.* x for various small times, as listed in the figure caption. The position of the front at each time, calculated using the exact solution (4.5b), is marked by a vertical line from $C = 0$ to $C = C_*$. The parameters chosen are as in (3.27a) with the additional choice of

$$k_0 = 4. \tag{4.14}$$

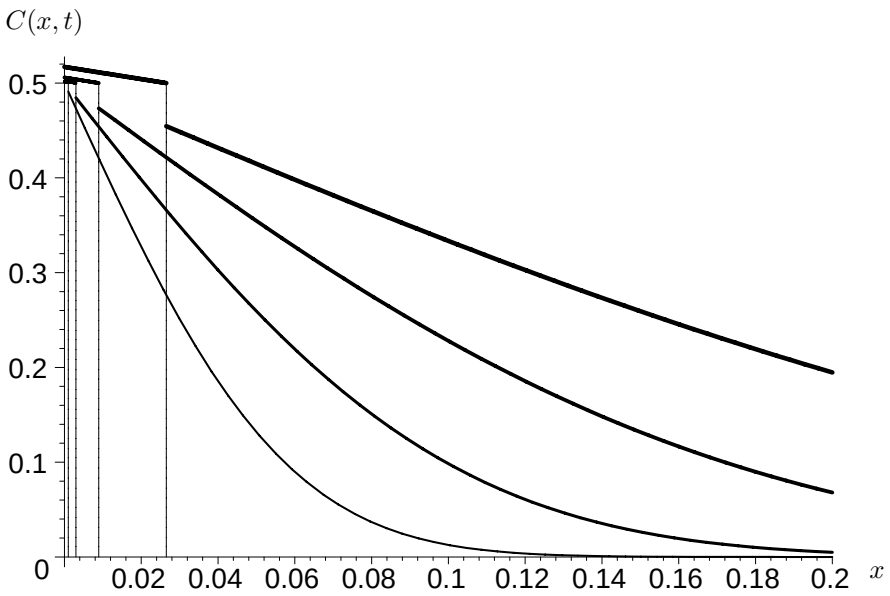

Figure 4.1.
In increasing order of thickness: $C(x,t)$ *vs.* x for $t = 0.001$, 0.03, 0.09, 0.27 and the parameters in (3.27) and (4.14).

The gaps in Fig. 4.1 occur because in the glassy region we are plotting the asymptotic solution given in (4.13), which has an $O(\sqrt{t})$ error. In contrast, there is no time-related error in the rubbery region solution, and hence $C^{0r}(s(t),t) = C_*$. We note that though the behavior is generally the same as in section 3, now the concentration at the boundary is nearly C_* and increases as a function of time. This is because the permeability is now lower, so the surface concentration is not immediately in equilibrium with the external environment. Again, we have a steady-state Fickian profile in the rubbery region matching to a purely Fickian profile in the glassy region.

4.2. Long-time asymptotics

Next we look at the solution for long time. Expanding (4.5a) for large time, we have

$$S(t) \sim \sqrt{2\frac{D_0(1-C_*)t}{a_0}} = 2b\sqrt{D_g t}, \quad t \to \infty. \tag{4.15}$$

Since (4.15) is the same as (3.24) with s replaced by S, in this regime our solution

is asymptotic to (3.26) with x replaced by $X = x + D_0/k_0$:

$$C_0^{\mathrm{g}}(x,t) \sim \frac{C_*}{\operatorname{erfc} b} \operatorname{erfc}\left(\frac{x + D_0/k_0}{2\sqrt{D_g t}}\right), \quad t \to \infty. \tag{4.16}$$

Rewriting (4.15) in the s notation, we have that

$$s(t) \sim -\frac{D_0}{k_0} + \sqrt{2\frac{D_0(1-C_*)t}{a_0}}, \quad t \to \infty. \tag{4.17}$$

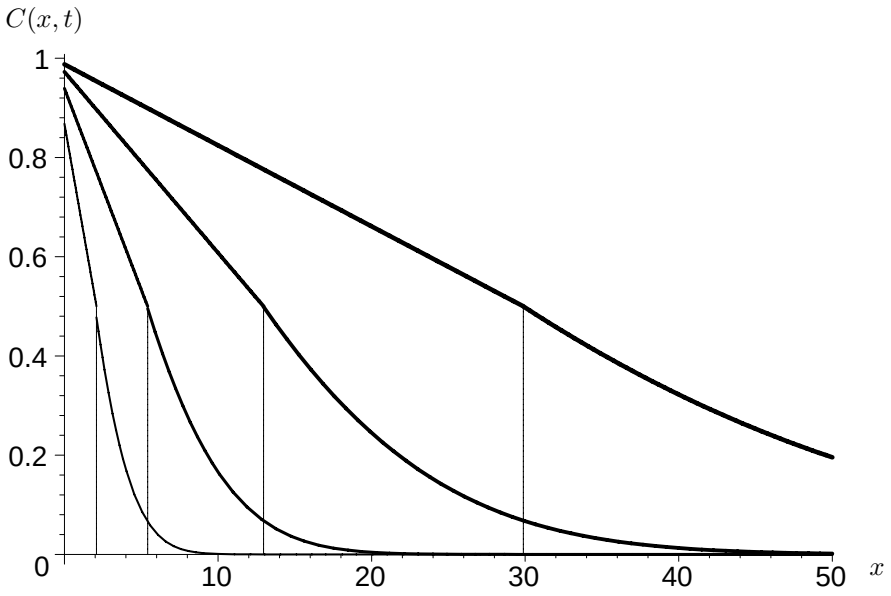

Figure 4.2.
In increasing order of thickness: $C(x,t)$ *vs.* x for $t = 5$, 25, 125, 625 and the parameters in (3.27) and (4.14).

Figure 4.2 shows a graph of the concentration *vs.* x for various large times, as indicated in the figure caption. The position of the front at each time, calculated using the exact solution (4.5b), is marked by a vertical line from $C = 0$ to $C = C_*$. The figure uses the parameters in (3.27) and (4.14). Note that as t gets large the surface concentration $C(0,t)$ has nearly equilibrated to the external concentration 1.

Figure 4.3 shows how the true solution for the front, given by (4.5b), compares with the asymptotic approximations in (4.12) and (4.17). The graph is on a log-lin scale. Note the close agreement of both approximations, especially the large-time approximation, which is virtually indistinguishable from the the actual front position.

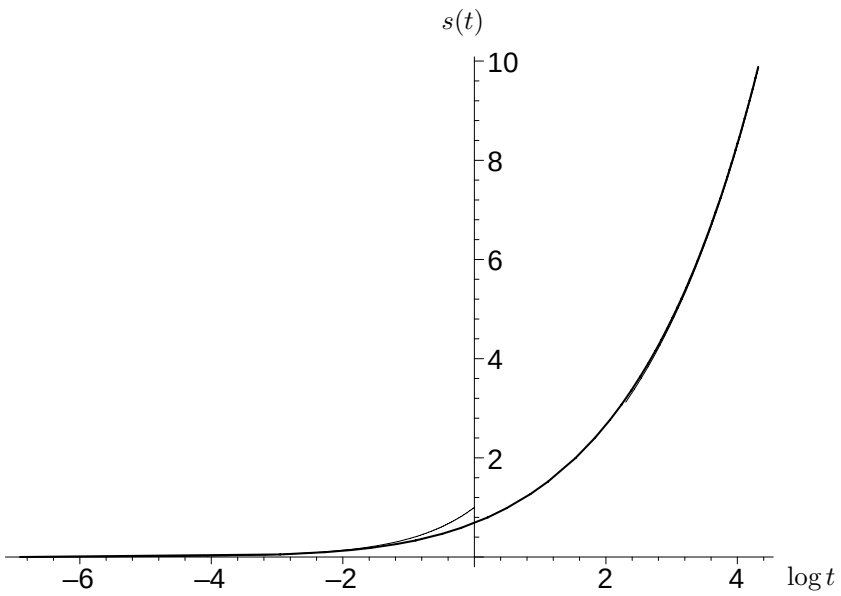

Figure 4.3.
$s(t)$ (thick line) and its short- and long-time approximations *vs.* $\log t$.

5. Stopping fronts

Next we wish to see what happens to this system on a longer time scale. Motivated by this goal, we note that since the length of a stretched polymer chain is on the order of hundreds of angstroms [11] and hence physically realizable, it is reasonable to use β_{r} to normalize our length scale. Note that this also introduces a longer time scale, and thus we rewrite our time variable as τ, which has the value ϵt. Making these substitutions into (2.15) and (2.22), we obtain

$$\frac{\partial^2 \sigma}{\partial x^2} - \frac{\beta^2(C)}{\beta_{\mathrm{r}}^2}\sigma = -\frac{\gamma\beta(C)}{\beta_{\mathrm{r}}}C + \frac{\beta(C)}{\beta_{\mathrm{r}}}\frac{\partial C}{\partial x}, \tag{5.1a}$$

$$\frac{\partial^3 C}{\partial x^2 \partial \tau} = D(C)\frac{\partial^4 C}{\partial x^4} - \frac{\gamma\beta(C)}{\beta_{\mathrm{r}}}\frac{\partial^2 C}{\partial x^2} + \frac{\beta(C)}{\beta_{\mathrm{r}}}\frac{\partial^3 C}{\partial x^3} + \frac{\beta^2(C)}{\beta_{\mathrm{r}}^2}\frac{\partial C}{\partial \tau} - \frac{\beta^2(C)D(C)}{\beta_{\mathrm{r}}^2}\frac{\partial^2 C}{\partial x^2}. \tag{5.1b}$$

Making the same parameter substitutions as in section 3 into (5.1), we have the following:

$$\frac{\partial^2 \sigma^{\mathrm{r}}}{\partial x^2} - \sigma^{\mathrm{r}} = -\gamma C^{\mathrm{r}} + \frac{\partial C^{\mathrm{r}}}{\partial x}, \tag{5.2a}$$

$$\frac{\partial^3 C^{\mathrm{r}}}{\partial x^2 \partial \tau} = D_0\epsilon^{-1}\frac{\partial^4 C^{\mathrm{g}}}{\partial x^4} - \gamma\frac{\partial^2 C^{\mathrm{g}}}{\partial x^2} + \frac{\partial^3 C^{\mathrm{g}}}{\partial x^3} + \frac{\partial C^{\mathrm{g}}}{\partial \tau} - D_0\epsilon^{-1}\frac{\partial^2 C^{\mathrm{g}}}{\partial x^2}, \tag{5.2b}$$

$$\frac{\partial^2 \sigma^{\mathrm{g}}}{\partial x^2} - \epsilon^{-2}\sigma^{\mathrm{g}} = \epsilon^{-1}\left(-\gamma C^{\mathrm{r}} + \frac{\partial C^{\mathrm{r}}}{\partial x}\right), \tag{5.3a}$$

$$\frac{\partial^3 C^{\mathrm{g}}}{\partial x^2 \partial \tau} = D_{\mathrm{g}}\frac{\partial^4 C^{\mathrm{g}}}{\partial x^4} - \gamma\epsilon^{-1}\frac{\partial^2 C^{\mathrm{g}}}{\partial x^2} + \epsilon^{-1}\frac{\partial^3 C^{\mathrm{g}}}{\partial x^3} + \epsilon^{-2}\frac{\partial C^{\mathrm{g}}}{\partial \tau} - D_{\mathrm{g}}\epsilon^{-2}\frac{\partial^2 C^{\mathrm{g}}}{\partial x^2}. \tag{5.3b}$$

Many of the other equations from section 3 do not depend on the choice of β_{c}, and hence remain the same with t replaced by τ.

5.1. The rubbery region and glassy pseudostress

In particular, if we assume a series in ϵ for our solutions as in (3.10), but with t replaced by τ, we see that (3.11) and (3.12) still hold. Thus we have that our solution is given by (3.13) with t replaced by τ:

$$C_0^{\mathrm{r}}(x,\tau) = 1 - \frac{(1-C_*)x}{s}. \tag{5.4}$$

Substituting (3.10) and (5.4) into (5.2a), we obtain

$$\frac{\partial^2 \sigma_0^{\mathrm{r}}}{\partial x^2} - \sigma_0^{\mathrm{r}} = -\gamma + \frac{(1-C_*)(\gamma x - 1)}{s},$$

the solution of which is

$$\sigma_0^{\mathrm{r}}(x,\tau) = \gamma - \frac{(1-C_*)(\gamma x-1)}{s} + \frac{\sinh x}{\sinh s}\left[\sigma_* - \gamma C_* - \frac{(1-C_*)}{s}\right] + \frac{\sinh(s-x)}{\sinh s}\left[\sigma_{\mathrm{b}}(t) - \gamma - \frac{(1-C_*)}{s}\right]. \tag{5.5}$$

In the glassy region, we assume a perturbation series for our solutions as in (3.16), but with t replaced by τ. In this case, the leading order of (5.3a) becomes $\sigma_0^{\mathrm{g}} = 0$, and hence an interior layer is needed. Since (3.5a) and the solution for σ_0^{g} still hold, the equations for the concentration must be as in section 3, except our expression for s will now be different. For the interior layer, the only difference is that since (5.3a) has an ϵ^{-2} term in it, our interior-layer variable must be

$$\zeta = \frac{x - s(t)}{\epsilon}.$$

Using this scaling, we obtain the same dominant balance in (5.3a) as in section 3. Thus

$$\sigma^{+}(\zeta,\tau) = \sigma_* e^{-\zeta}, \tag{5.6}$$

as before.

5.2. The front position

Due to the narrower interior layer on this time scale, the pseudostress now contributes to the front condition (3.7). Using our boundary-layer scalings, we obtain, to leading order,

$$-\sigma_* + D_0 \frac{(1-C_*)}{s} = a_0 \dot{s}, \tag{5.7}$$

where we have used (5.4) and (5.6) and the dot now indicates differentiation with respect to τ. Integrating, we have

$$\frac{\sigma_* \tau}{a_0} = -s - \frac{D_0(1-C_*)}{\sigma_*} \log\left(1 - \frac{s\sigma_*}{D_0(1-C_*)}\right), \tag{5.8}$$

where we have used (3.9), which also holds on the τ time scale. Equation (5.8) gives s implicitly as a function of τ. However, it will often be more convenient to work with (5.7) directly.

We note from (5.8) that

$$s(\tau) \leq \frac{D_0(1-C_*)}{\sigma_*} \equiv s_\infty \tag{5.9}$$

for all τ. Therefore, we see that this front will stop at the finite location s_∞, which is independent of a_0, which relates the flux differential to the front speed. This behavior is in sharp contrast to the usual models involving viscoelastic memory effects [31], [32], since in that case the stress would have to decay away to zero in order to maintain equilibrium at a stopping front. Since the stress usually remains of one sign and is a hereditary effect, that will not occur in such models.

However, in our model a stopping front may be maintained by a nonzero pseudostress. In particular, we see that since the polymer is in effect equilibrated to leading order in the rubbery region, on a slow time scale there will not be a large enough flux to overcome the differential $a_0\dot{s}$, and hence the front will stop. When the diffusion in the rubbery region is weak (D_0 is small), the exterior concentration is near the rubber-glass transition ($1-C_*$ is small), or the pseudostress at the interface σ_* is large, then the front will not penetrate very far into the polymer, and conversely. Rewriting (5.8) using our definition of s_∞, we obtain

$$\frac{\sigma_* \tau}{a_0} = -s - s_\infty \log\left(1 - \frac{s}{s_\infty}\right). \tag{5.10}$$

Figure 5.1 shows a graph of the pseudostress *vs.x* for various times, which are listed in the figure caption. The position of the front at each time, calculated using the exact solution (5.10), is marked by a vertical line from $\sigma = 0$ to $\sigma = \sigma_*$. With these parameters, we see that $s_\infty = 9/4$. We note that we have a peak in the pseudostress in the rubbery region behind the front. This type of behavior

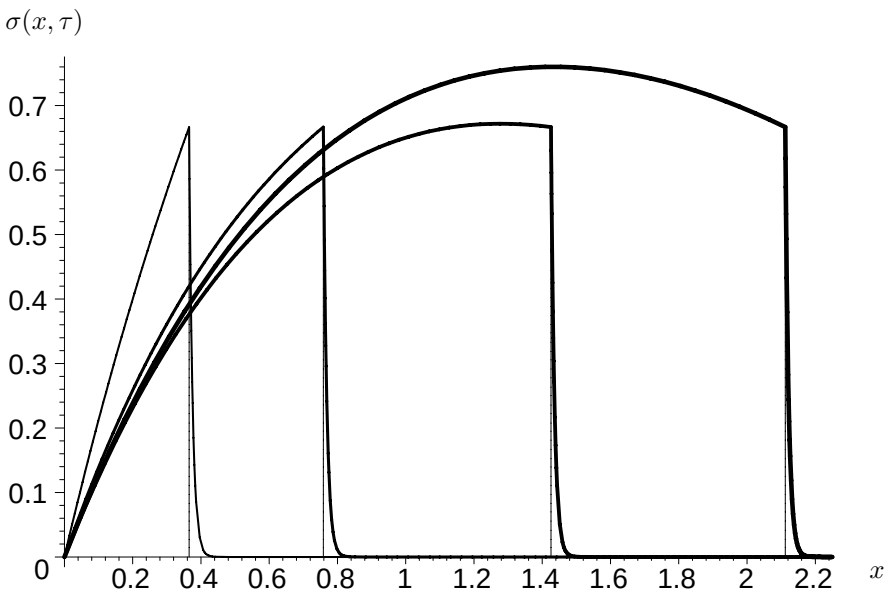

Figure 5.1.
In increasing order of thickness: $\sigma(x,\tau)$ *vs.* x for $\tau = 0.1$, 0.5, 2.5, and 12.5 and the parameters in (3.27) and (4.14).

has been seen in the stress in viscoelastic models, but previously only in a region localized near the front [24]. We note that each of the terms in (5.5) remains bounded as $\tau \to \infty$, so the peak asymptotes to a finite value.

Physically, σ builds up more quickly in the rubbery region than can be adequately dispersed in the glassy region. This sort of "overshoot" has been seen in the concentration profiles in these sorts of polymer-penetrant systems [23].

6. Asymptotics

We now turn to the last part of our analysis: the study of C_0^{g}. As mentioned in the previous section, the solution is governed by (3.18), (3.19), and (3.25) with t replaced by τ. However, as in section 4 there is not a simple expression for $s(\tau)$, and so we must use Boley's method. The solution is given by (4.10) with t replaced by τ.

6.1. Small-time asymptotics

We begin with small-time asymptotics. Letting

$$s(\tau) \sim s_0 \tau^{\alpha}, \qquad \tau \to 0; \quad \alpha > 0, \tag{6.1}$$

in (5.7), we obtain

$$-\sigma_* + D_0 \frac{(1 - C_*)}{s_0 \tau^{\alpha}} = a_0 s_0 \alpha \tau^{\alpha - 1},$$

and thus the leading-order balance is given by $\alpha = 1/2$. Substituting this into the above, we have the following:

$$s(\tau) = 2b\sqrt{D_{\mathrm{g}}\tau}, \quad \tau \to 0, \tag{6.2}$$

as in (3.24). Therefore, our solution for small time is given by (3.26) with t replaced by τ:

$$C_0^{\mathrm{g}}(x, \tau) = C_* \frac{\operatorname{erfc}(x/2\sqrt{D_g \tau})}{\operatorname{erfc} b}, \quad \tau \to 0. \tag{6.3}$$

The reason why (6.2) and (6.3) should hold can best be explained using the theory of matched asymptotic expansions. Since t is essentially an initial-layer variable for τ, the behavior of the functions s and C_0^{g} as $\tau \to 0$ should exactly match those in section 3 as $t \to \infty$.

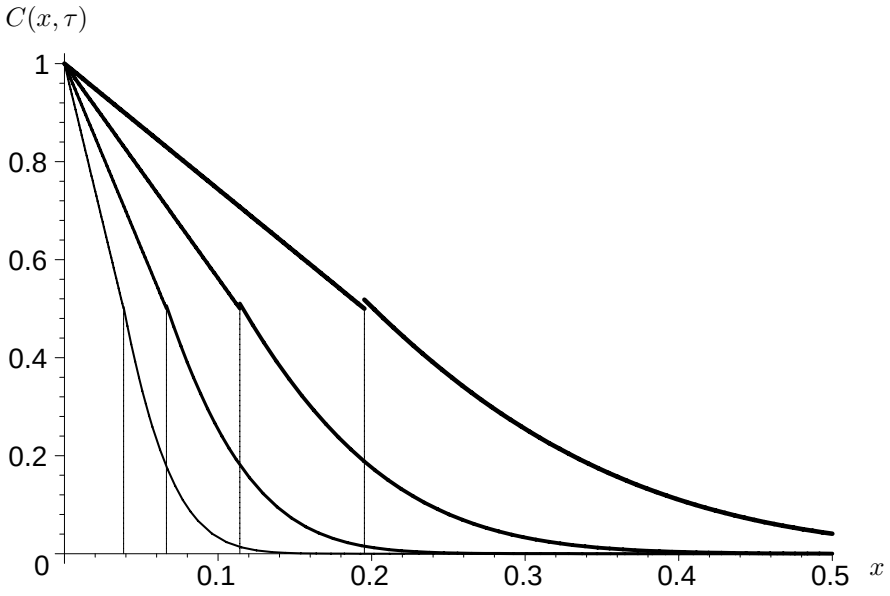

Figure 6.1.
In increasing order of thickness: $C(x, \tau)$ *vs.* x for $\tau = 0.01$, 0.03, 0.09, and 0.27 and the parameters in (3.27) and (4.14).

Figure 6.1 shows a graph of the concentration *vs.* x for the small-time values shown in the figure caption. The position of the front at each time, calculated using the exact solution (5.10), is marked by a vertical line from $C = 0$ to $C = C_*$. Here the solution in the rubbery region is exact as given in (5.4), while the solution in the glassy region is the asymptotic approximation in (6.3). (This explains the small gap in the solution for the larger τ values.) Note that the solution looks nearly Fickian, due to the smaller width of the rubbery region where the nonlocality is greater. Again, behind the front we have a steady-state Fickian profile due to the greater equilibration in the rubbery region.

6.2. Long-time asymptotics

Next we examine the front position for large time. Motivated by (5.9), we let

$$s(\tau) \sim s_\infty \left[1 - s_\Delta(\tau)\right], \quad \tau \to \infty, \tag{6.4}$$

where $s_\Delta(\tau) \to 0^+$ as $\tau \to \infty$. Substituting (6.4) into (5.10), we obtain, to leading order,

$$s_\Delta(\tau) = \exp\left(-1 - \frac{\sigma_* \tau}{a_0 s_\infty}\right). \tag{6.5}$$

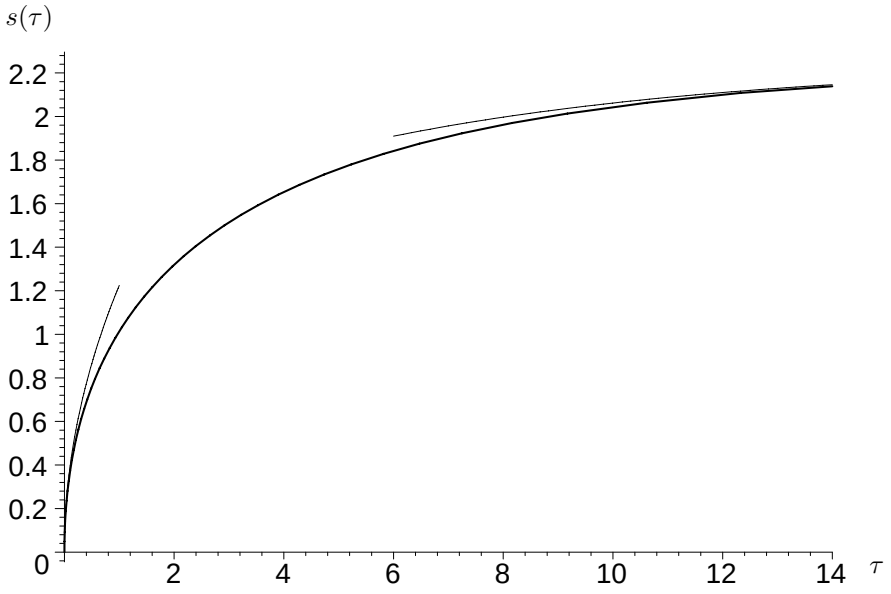

Figure 6.2.
$s(\tau)$ (thick line) and its short- and long-time approximations *vs.* τ.

Figure 6.2 shows how the true solution for the front, given by (5.10), compares with the asymptotic approximations in (6.2) and (6.4). Note the close agreement of both approximations in their regions of validity.

Since $s(\tau)$ approaches a constant as $\tau \to \infty$, it is more convenient to introduce the new variables

$$\xi = x - s_\infty, \qquad T(x,\tau) = T_\infty(\xi,\tau), \tag{6.6}$$

into (4.6)–(4.9). In particular, (4.6) becomes

$$T_\infty(0,\tau) = f_{\mathrm{b}}(\tau). \tag{6.7}$$

Since the operators are invariant under translation, we obtain the same solution as in (4.10) for T_∞. However, there is one minor point regarding (6.7) that must be addressed.

With the change in variables in (6.6), $T_\infty(\xi,\tau)$ and C_0^{g} agree in the range $\xi > s(\tau) - s_\infty$. Since the right-hand side is always negative, we see that the line $\xi = 0$ where we impose our FBC $f_{\mathrm{b}}(\tau)$ in (6.7) is now *interior* to the domain. However, this is not a concern since the positioning of the fictitious condition is chosen in order to simplify the algebra.

Our front condition (4.9) is now given by

$$T_\infty(-s_\infty s_\Delta(\tau),\tau) = C_*,$$

which can be approximated using the smallness of s_Δ as

$$f_{\mathrm{b}}(\tau) - s_\infty s_\Delta(\tau)\frac{\partial T_\infty}{\partial \xi}(0,\tau) = C_*, \tag{6.8}$$

where we have used (6.7).

Motivated by (6.8), we write

$$f_{\mathrm{b}}(\tau) = C_* + f_\Delta(\tau), \tag{6.9}$$

where $f_\Delta(\tau) \to 0$ as $\tau \to \infty$. Clearly (6.9) satisfies (6.8) as $\tau \to \infty$. Substituting (6.9) into (4.10), we obtain

$$T_\infty(\xi,\tau) = C_* \operatorname{erfc}\left(\frac{\xi}{2\sqrt{D_{\mathrm{g}}\tau}}\right) + T_\Delta(\xi,\tau), \tag{6.10a}$$

$$T_\Delta(\xi,\tau) = \frac{\xi}{2\sqrt{\pi D_{\mathrm{g}}}}\int_0^\tau \frac{f_\Delta(z)}{(\tau-z)^{3/2}} \exp\left[-\frac{\xi^2}{4D_{\mathrm{g}}(\tau-z)}\right] dz. \tag{6.10b}$$

Taking the derivative of (6.10) and retaining only the leading-order terms yields

$$\frac{\partial T_\infty}{\partial \xi}(0,\tau) = -\frac{C_*}{\sqrt{\pi D_{\mathrm{g}}\tau}}. \tag{6.11}$$

Substituting (6.9) and (6.11) into (6.8), solving for $f_\Delta(\tau)$, and using the result in (6.10), we have the following:

$$T_\Delta(\xi,\tau) = -\frac{s_\infty C_*}{e\sqrt{\pi D_\mathrm{g}}}\times \left\{\frac{\xi}{2\sqrt{\pi D_\mathrm{g}}}\int_0^\tau \exp\left(-\frac{\sigma_* z}{a_0 s_\infty}\right)\frac{1}{(\tau-z)^{3/2}\sqrt{z}}\exp\left[-\frac{\xi^2}{4D_\mathrm{g}(\tau-z)}\right]\,dz\right\}. \quad (6.12)$$

We wish to find an asymptotic formula for $T_\Delta(\xi,\tau)$ which is valid as $\tau\to\infty$. There is no local maximum in the arguments of the exponentials in the integrand, but a plot of the integrand confirms that the dominant contributions are from the endpoints. At $z=\tau$, both the exponentials become transcendentally small, while at $z=0$, the exponentials are $O(1)$. Hence we also expand (6.12) about $z=0$:

$$T_\Delta(\xi,\tau) \sim -\frac{s_\infty C_* \xi}{2D_\mathrm{g}}\sqrt{\frac{a_0 s_\infty}{\sigma_*\pi\tau^3}}\exp\left(-1-\frac{\xi^2}{4D_\mathrm{g}\tau}\right)\mathrm{erf}\left(\sqrt{\frac{\sigma_*\tau}{a_0 s_\infty}}\right). \quad (6.13a)$$

However, we note that (6.13a) does not satisfy (6.7). This is due to the fact that for small ξ, the second exponential in (6.12) becomes small *slowly*. Therefore, we expand (6.12) about $z=\tau$:

$$T_\Delta(\xi,\tau) \sim -\frac{s_\infty C_*}{e\sqrt{\pi D_\mathrm{g}\tau}}\exp\left(-\frac{\sigma_*\tau}{a_0 s_\infty}\right)\mathrm{erfc}\left(\frac{\xi}{2\sqrt{D_\mathrm{g}\tau}}\right). \quad (6.13b)$$

Equation (6.13b) does satisfy (6.7). We note that if we add them together, we obtain a uniform expansion, since in any region away from $\xi=0$ (6.13a) is transcendentally small when compared with (6.13b). Near $\xi=0$, (6.13b) is $O(\xi/\tau)$ smaller than (6.13a).

Therefore, we have that

$$T_\infty(\xi,\tau) = C_*\,\mathrm{erfc}\left(\frac{\xi}{2\sqrt{D_\mathrm{g}\tau}}\right) - \frac{s_\infty C_*}{e\sqrt{\pi D_\mathrm{g}\tau}}\left\{\frac{\xi}{\tau}\sqrt{\frac{a_0 s_\infty}{\sigma_* D_\mathrm{g}}}\exp\left(-\frac{\xi^2}{4D_\mathrm{g}\tau}\right)\mathrm{erf}\left(\sqrt{\frac{\sigma_*\tau}{a_0 s_\infty}}\right) + \exp\left(-\frac{\sigma_*\tau}{a_0 s_\infty}\right)\mathrm{erfc}\left(\frac{\xi}{2\sqrt{D_\mathrm{g}\tau}}\right)\right\}, \quad (6.14)$$

where we have used (6.10a).

Figure 6.3 shows a graph of the concentration *vs.* x for the large-time values shown in the figure caption. The position of the front at each time, calculated using (5.10), is marked by a vertical line from $C=0$ to $C=C_*$. Here the solution

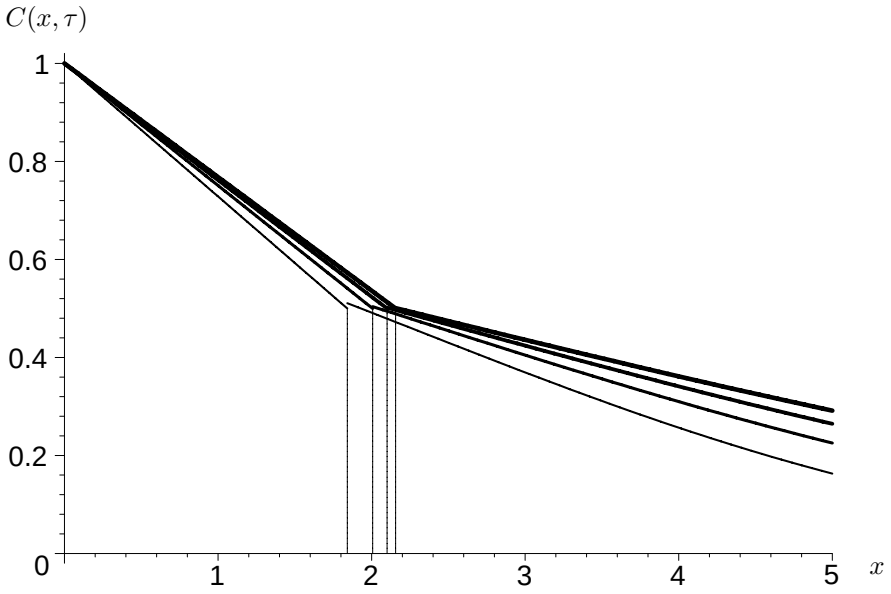

Figure 6.3.
In increasing order of thickness: $C(x,\tau)$ *vs.* x for $\tau = 3$, 6, 12, and 15 and the parameters in (3.27) and (4.14).

in the rubbery region is exact as given in (5.4), while the solution in the glassy region is the asymptotic approximation in (6.14). (This explains the small gap in the solution for $\tau = 3$.) Note that though the time values increase linearly, the front position slows as it approaches its limiting value 9/4. Note also that the solution in the glassy region is nearly linear, indicating the near steady-state behavior of the function.

Some discussion of s_∞ is appropriate. We note that in this case s_∞ is only a few times the characteristic length of a polymer chain in the rubbery state. However, due to the entangled nature of the polymer network, even at such a small depth there will be a great many "pockets" through which the penetrant diffuses.

7. Lower permeability

Now we examine the case where the permeability is not quite so large. We again assume that $k = k_0\epsilon^{-1}$. Since the only dependence of (4.3) on t is through s, equation (4.3) also holds on the τ time scale:

$$C_0^{\mathrm{r}}(x,\tau) = C_* + \frac{k_0 s(1-C_*)}{k_0 s + D_0}\left(1 - \frac{x}{s}\right). \tag{7.1}$$

Note that in the limit that $k_0 \to \infty$, (7.1) reduces to (5.4).

Substituting (7.1) into (5.2a), we have the following:

$$\frac{\partial^2 \sigma_0^{\mathrm{r}}}{\partial x^2} - \sigma_0^{\mathrm{r}} = -\gamma\left[C_* + \frac{k_0 s(1-C_*)}{k_0 s + D_0}\left(1 - \frac{x}{s}\right)\right] - \frac{k_0(1-C_*)}{k_0 s + D_0},$$

the solution of which is

$$\begin{aligned}\sigma_0^{\mathrm{r}}(x,\tau) &= \gamma\left[C_* + \frac{k_0 s(1-C_*)}{k_0 s + D_0}\right]\left[1 - \frac{\sinh(s-x)}{\sinh s}\right] - \frac{k_0(1-C_*)(\gamma x - 1)}{k_0 s + D_0} \\ &+ \frac{\sinh x}{\sinh s}\left[\sigma_* - \gamma C_* - \frac{k_0(1-C_*)}{k_0 s + D_0}\right] + \frac{\sinh(s-x)}{\sinh s}\left[\sigma_{\mathrm{b}}(\tau) - \frac{k_0(1-C_*)}{k_0 s + D_0}\right]. \end{aligned} \tag{7.2}$$

Our work from section 5 for the glassy region remains unchanged, and hence we may substitute (7.2) and (5.6) into (3.7) to obtain

$$-\sigma_* + \frac{D_0(1-C_*)}{S} = a_0\dot{S}, \tag{7.3}$$

where S is defined as in section 4. But we note that the operator in (7.3) is the same as the operator in (5.7), except now the operator holds for S. Solving, we have

$$\frac{\sigma_*\tau}{a_0} = -s - s_\infty \log\left(1 - \frac{s}{s_\infty - D_0/k_0}\right). \tag{7.4}$$

Note that in the limit that $k_0 \to \infty$, (7.4) reduces to (5.10).

It is clear that if s ever equals $s_\infty - D_0/k_0$, the front will stop. (This is equivalent to $S = s_\infty$.) Therefore, we define $u_\infty = s_\infty - D_0/k_0$, so (7.4) becomes

$$\frac{\sigma_*\tau}{a_0} = -s - s_\infty \log\left(1 - \frac{s}{u_\infty}\right). \tag{7.5}$$

We now note that there are two distinct cases, depending on the sign of u_∞. We begin by examining the small-time asymptotics. Substituting (6.1) into (7.3), we obtain

$$-\sigma_* + k_0(1-C_*)\left(1 - \frac{k_0 s_0 \tau^\alpha}{D_0}\right) = a_0 s_0 \alpha \tau^{\alpha-1},$$

which implies that $\alpha = 1$ and

$$-\sigma_* + k_0(1 - C_*) = a_0 s_0. \tag{7.6}$$

However, now we note a problem. If $u_\infty < 0$, this implies that

$$k_0(1 - C_*) < \sigma_*, \tag{7.7}$$

and hence the right-hand side of (7.6) is negative, implying a front that moves to the left. The physical interpretation can be gleaned from (7.7). In this case, the permeability is so low that the amount of penetrant allowed into the matrix cannot surmount the flux barrier given by the a_0 term in (7.6). Therefore, we now focus on the case where $s_\infty - D_0/k_0 > 0$.

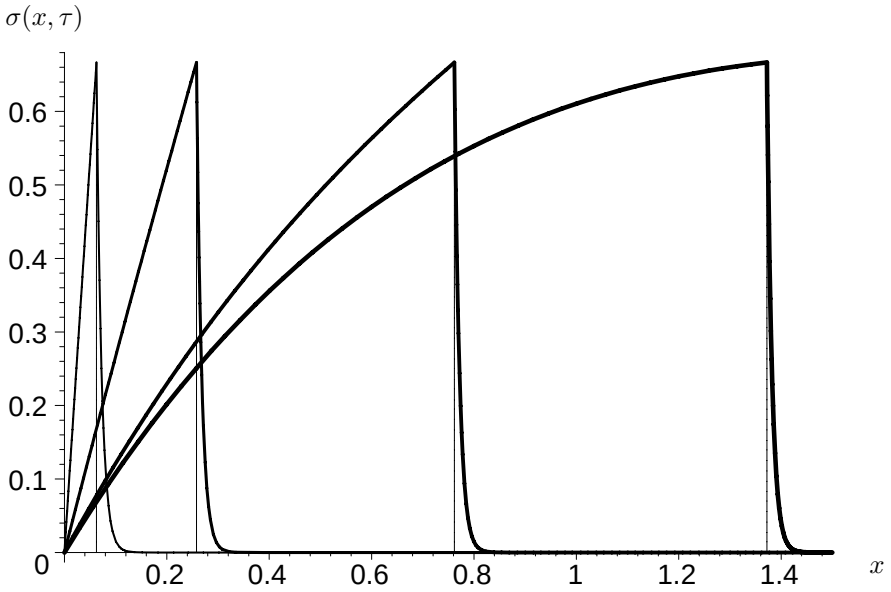

Figure 7.1.
In increasing order of thickness: $\sigma(x, \tau)$ *vs.* x for $\tau = 0.1$, 0.5, 2.5, and 12.5 and the parameters in (3.27) and (4.14).

Figure 7.1 shows a graph of the pseudostress *vs.* x for various times, which are listed in the figure caption. The position of the front at each time, calculated using the exact solution (7.5), is marked by a vertical line from $\sigma = 0$ to $\sigma = \sigma_*$. We note that the peak that developed in section 5 has not developed here. Due to the boundary condition (4.2), the surface concentration starts out at C_* and only eventually asymptotes to 1. Therefore, σ does not increase as quickly in the rubbery region.

Continuing to solve (7.6), we see that

$$s(\tau) \sim \frac{[k_0(1-C_*)-\sigma_*]\tau}{a_0}, \quad \tau \to 0. \tag{7.8}$$

We note that the front moves more slowly now since the permeability is smaller. Since the front moves more slowly than $\sqrt{\tau}$, we may again assume a form for $f_{\mathrm{b}}(\tau)$ that approaches a nonzero constant as $\tau \to 0$. Thus, we again obtain (4.13) with t replaced by τ:

$$C_0^{\mathrm{g}}(x,\tau) \sim C_* \operatorname{erfc}\left(\frac{x}{2\sqrt{D_{\mathrm{g}}\tau}}\right), \quad \tau \to 0. \tag{7.9}$$

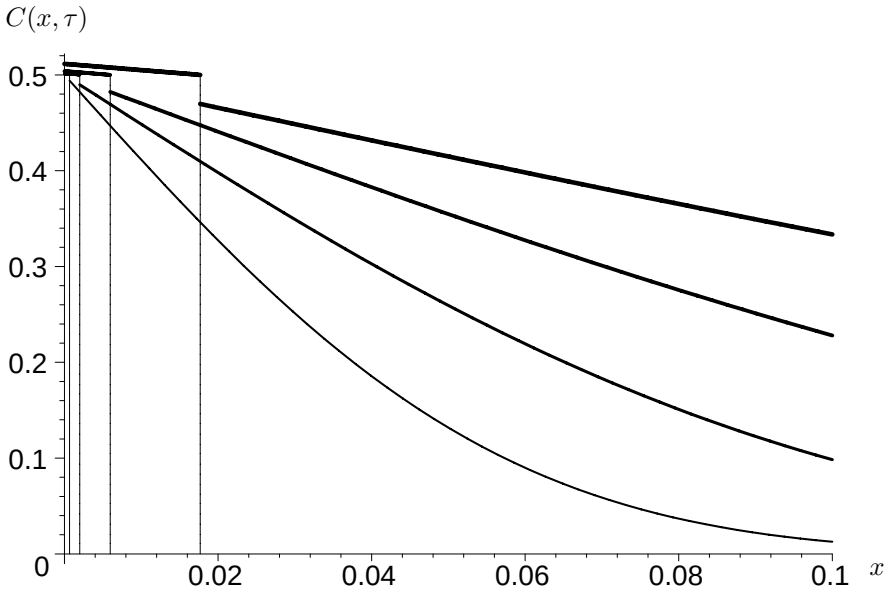

Figure 7.2.
In increasing order of thickness: $C(x,\tau)$ *vs.* x for $\tau = 0.01$, 0.03, 0.09, and 0.27 and the parameters in (3.27) and (4.14).

Figure 7.2 shows a graph of the concentration *vs.* x for the small-time values shown in the figure caption. The position of the front at each time, calculated using the exact solution (7.5), is marked by a vertical line from $C = 0$ to $C = C_*$. Here the solution in the rubbery region is exact as given in (7.1), while the solution in the glassy region is the asymptotic approximation in (7.9). (This explains the gap in the solution for the larger τ values.) As mentioned earlier, we see that the surface concentration is very near $C = C_*$ in this time regime.

To do the long-time asymptotics, we redefine s_Δ in the following manner:

$$s(\tau) \sim u_\infty \left[1 - s_\Delta(\tau)\right], \quad \tau \to \infty. \tag{7.10}$$

(Here it becomes clear why there is no solution if $u_\infty < 0$.) Substituting (7.10) into (7.5) and using the smallness of s_Δ, we obtain

$$s_\Delta(\tau) = \exp\left(-\frac{u_\infty}{s_\infty} - \frac{\sigma_* \tau}{a_0 s_\infty}\right). \tag{7.11}$$

Note that in the limit that $k_0 \to \infty$, (7.11) reduces to (6.5).

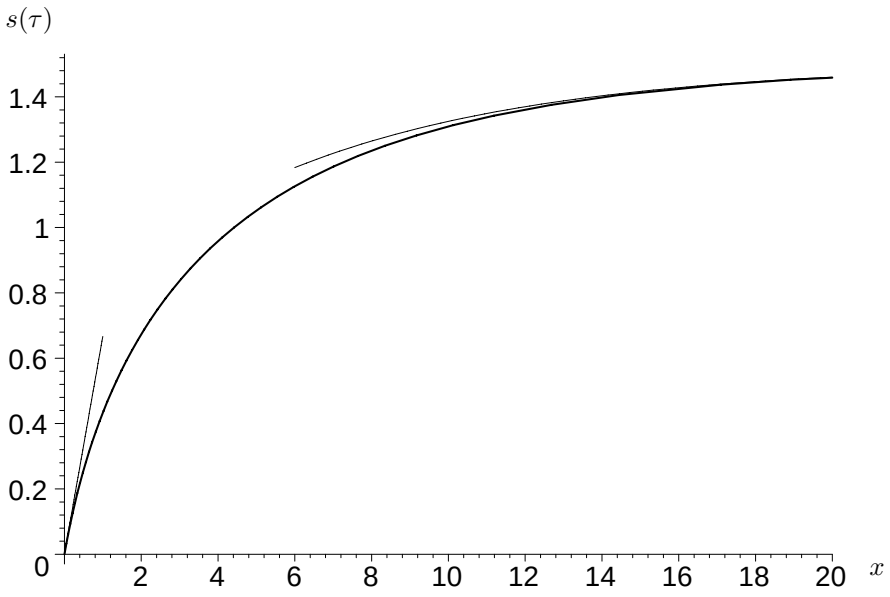

Figure 7.3.
$s(\tau)$ (thick line) and its short- and long-time approximations *vs.* τ.

Figure 7.3 shows how the true solution for the front, given by (7.5), compares with the asymptotic approximations in (7.8) and (7.10). Note the close agreement of both approximations in their regions of validity.

If we replace the definition of ξ in (6.6) by

$$\xi = x - u_\infty, \tag{7.12}$$

the solution process for T_∞ proceeds as before, with f_Δ being given by

$$f_\Delta(\tau) = -u_\infty \frac{C_*}{\sqrt{\pi D_g \tau}} \exp\left(-\frac{u_\infty}{s_\infty} - \frac{\sigma_* \tau}{a_0 s_\infty}\right), \tag{7.13}$$

where we have used (7.11).

Keeping close track of which of the s_∞ remain and which get changed to u_∞, it is relatively straightforward to see that equation (6.14) is replaced by

$$T_\infty(\xi,\tau) = C_* \operatorname{erfc}\left(\frac{\xi}{2\sqrt{D_g\tau}}\right) - \frac{u_\infty C_* e^{-u_\infty/s_\infty}}{\sqrt{\pi D_g\tau}} \times \left\{\frac{\xi}{\tau}\sqrt{\frac{a_0 s_\infty}{\sigma_* D_g}} \exp\left(-\frac{\xi^2}{4D_g\tau}\right) \operatorname{erf}\left(\sqrt{\frac{\sigma_*\tau}{a_0 s_\infty}}\right) + \exp\left(-\frac{\sigma_*\tau}{a_0 s_\infty}\right) \operatorname{erfc}\left(\frac{\xi}{2\sqrt{D_g\tau}}\right)\right\}. \tag{7.14}$$

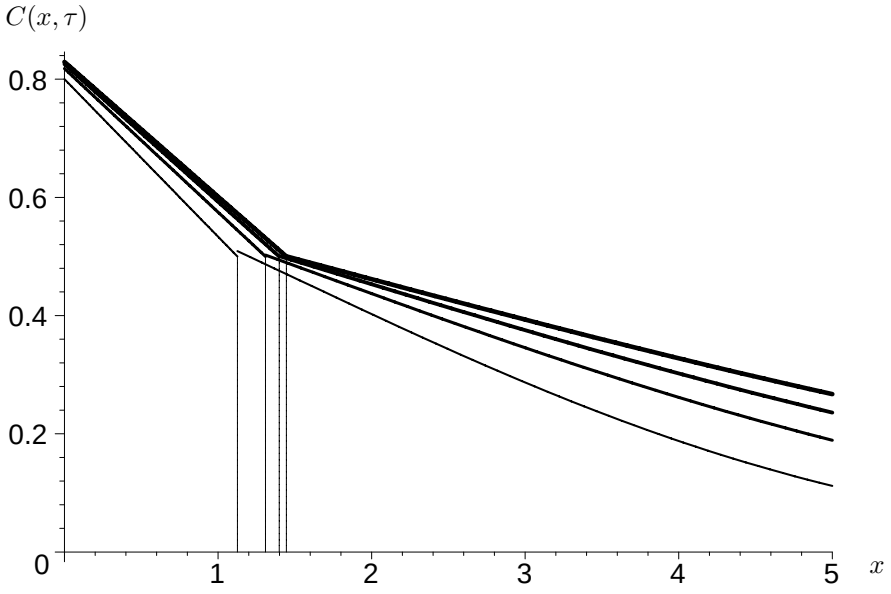

Figure 7.4.
In increasing order of thickness: $C(x,\tau)$ *vs.* x for $\tau = 6$, 10, 14, 18, and the parameters in (3.27) and (4.14).

Figure 7.4 shows a graph of the concentration *vs.*x for the large-time values shown in the figure caption. The position of the front at each time, calculated using the exact solution (7.5), is marked by a vertical line from $C = 0$ to $C = C_*$. Here the solution in the rubbery region is exact as given in (7.1), while the solution in the glassy region is the asymptotic approximation in (7.14). (This explains the small gap in the solution for $\tau = 6$.) Note that though the time values increase linearly, the front position slows as it approaches its limiting value 9/4. Note also

that the solution in the glassy region is nearly linear, indicating the near steady-state behavior of the function. Note that as τ gets large the surface concentration $C(0,\tau)$ has nearly equilibrated to the external concentration 1.

8. Conclusions

Penetrant diffusion in polymers cannot be described by Fick's Law alone. It has become common to model such nonstandard effects by considering the polymer entanglement network as a viscoelastic material and introducing a relaxation time [2], [33], [34]. This introduces a nonlocal effect in time *via* the introduction of a hereditary integral [4], [5]. However, due to the morphology of the network, it is also reasonable to include nonlocal spatial behavior to model the nonstandard effects.

Following the reasoning in [7], we postulate that the chemical potential depends not only on the concentration $\tilde{C}$, but also on the pseudostress $\tilde{\sigma}$, which incorporates the nonlocal spatial effects. In so doing we obtain a single partial integrodifferential equation which can be split into a set of two coupled partial differential equations. With further physically reasonable assumptions, the model may be reduced to one fourth-order partial differential equation.

These assumptions necessitated stating the system as a moving boundary-value problem. The moving interface separated two zones where two different types of equations held: a steady-state Fickian operator for the concentration in the rubbery region, and a standard Fickian operator for the concentration in the glassy region. The equations for the pseudostress varied with the characteristic scales chosen. When scaling, we related the characteristic length and time scales, thus creating a system where rescaling one forced the rescaling of the other.

We solved the resulting problem on two different time scales and with two different radiation conditions. On the faster time scale with a highly permeable exposed surface, the front moves in a purely Fickian way. The concentration in the rubbery region exhibits a linear profile, while Fickian profiles appear in the glassy region. This is due to the fact that in the glassy region the effects of the nonlocality are negligible (as seen in the leading-order value of zero in the pseudostress), while in the rubbery region the expansion and disentangling of the polymer entanglement network leads to a faster equilibration. This is confirmed by the nonzero value of the pseudostress in the glassy region.

With an $O(1)$ balance in the radiation condition, the front still moves as if the problem were Fickian. It starts off more slowly, since there is a smaller concentration gradient at the surface. However, it quickly undergoes a transition to a Fickian profile at longer time scales. In this case, the concentration profiles can not be found explicitly, but by using an integral method due to Boley [29] we were able to construct long- and-short time asymptotic solutions.

On the longer time scale with a highly permeable exposed surface, we discov-

ered that the moving interface stopped as $\tau \to \infty$, decaying exponentially to an equilibrium value. This behavior has not been seen in viscoelastic models, and in our model is a direct result of the spatial form of the nonlocality. The concentration profiles again were steady-state Fickian and Fickian in the glassy and rubbery regions respectively, but the effect of the memory is enhanced due to the longer spatial scales considered. This buildup in the memory effect slows the front down, as seen previously [23], and the slowing front causes the pseudostress to bulge behind it, as shown in Fig. 5.1. The front may progress only a few characteristic lengths of the polymer strands, but due to the nature of the entanglement network, this may include a large number of pockets. To construct a uniformly long-time approximation to the integral solution resulting from Boley's method, the contributions from two points must be summed.

With an $O(1)$ balance in the radiation condition, the front will still stop, but there is a shift to the left in the front position. In order for the front actually to advance into the polymer, a condition on the permeability, given by (7.7), must hold. Due to the fact that the surface concentration increases slowly, no bulge in the pseudostress is seen.

Though this work obviously presents only one application of the new model, the behavior shown captures essential facets of the behavior of both the physical system and the viscoelastic model. However, in contrast to the viscoelastic models, the new model captures the behavior of stopping fronts, which appear in experiments of desorption in polymers [35]. In further work we will analyze the desorption and "skinning" problems directly, as well as sorption in other geometries.

Acknowledgments

Many of the calculations herein where checked using Maple. This work was supported by the University of Delaware Research Foundation and the National Science Foundation grant #DMS-9972013.

Nomenclature

Variables and Parameters

Units are listed in terms of length (L), mass (M), moles (N), or time (T). If the same letter appears both with and without tildes, the letter with a tilde has dimensions, while the letter without a tilde is nondimensionalized. The equation where a quantity first appears is listed, if appropriate.

$\tilde{a}$: coefficient in flux-front speed relationship, units N/L^3.
b: constant, defined in (3.24) as $[D_0(1-C_*)/(2a_0D_{\mathrm{g}})]^{1/2}$.
$\tilde{C}(\tilde{x},\tilde{t})$: concentration of penetrant or diluent at position $\tilde{x}$ and time $\tilde{t}$, units N/L^3.

$\tilde{D}(\tilde{C})$: binary diffusion coefficient for system, units L^2/T.
$E(\tilde{C})$: coefficient preceding the $\tilde{\sigma}$ term in the modified diffusion equation, units NT/M (2.5).
$f(\cdot)$: arbitrary function, variously defined (2.1).
$\tilde{J}(\tilde{x},\tilde{t})$: flux at position $\tilde{x}$ and time $\tilde{t}$, units N/L^2T (2.5).
$K(\tilde{C})$: nonlinear function of proportionality, units N^2T/ML^3 (2.5).
k: coefficient measuring permeability of exposed surface, units L/T (2.10).
$S(\cdot)$: shifted front position at time $\cdot$, value $s(\cdot)+D_0/k_0$ (4.4a).
$\tilde{s}(\tilde{t})$: position of rubber-glass transition front at time $\tilde{t}$, units L (2.11).
$T(\cdot,\cdot)$: fictitious representation of C_0^{g} used in Boley's method (4.6).
$\tilde{t}$: time from imposition of external concentration, units T.
u_∞: shifted front stopping position, value $s_\infty - D_0/k_0$ (7.5).
X: shifted spatial coordinate, value $x + D_0/k_0$.
$\tilde{x}$: spatial coordinate, units L (2.1).
$\mathcal{Z}$: the integers.
z: dummy variable (2.1).
α: arbitrary exponent, variously defined (6.1).
$\beta(\tilde{C})$: inverse of the dependence length, units L^{-1}.
γ: dimensionless parameter, value $\eta/\nu\beta_{\mathrm{r}}$ (3.3b).
ϵ: perturbation expansion parameter, value $\beta_{\mathrm{r}}/\beta_{\mathrm{g}}$.
ζ: dimensionless interior layer variable about glass-rubber interface (3.20).
η: coefficient of concentration in $\tilde{\sigma}$ evolution equation (2.3), units ML/NT^2.
ξ: shifted spatial coordinate (6.6).
$\tilde{\mu}$: chemical potential, units ML^2/T^2N.
ν: coefficient of $\partial\tilde{C}/\partial\tilde{t}$ in $\tilde{\sigma}$ evolution equation (2.3), units ML^2/NT^2.
$\tilde{\sigma}(\tilde{x},\tilde{t})$: memory term in flux at position $\tilde{x}$ and time $\tilde{t}$, units M/LT^2.
τ: compressed time variable, value ϵt.

Other notation

b: as a subscript, used to indicate the boundary $\tilde{x}=0$ (2.9).
c: as a subscript, used to indicate the characteristic value of a quantity (2.7).
ext: as a subscript, used to indicate the exterior ambient concentration (2.10).
g: as a sub- or superscript, used to indicate the glassy state (2.7).
$j \in \mathcal{Z}$: as a sub- or superscript, used to indicate a term in an expansion in ϵ.
r: as a sub- or superscript, used to indicate the rubbery state (2.7).
Δ: as a subscript, refers to the deviation from an asymptote (6.4).
$*$: as a subscript, used to indicate at the transition value between the glassy and rubbery states (2.7).
∞: as a subscript, used to indicate a limiting value as $\tau \to \infty$ (5.9).
$+$: as a superscript on σ, used to indicate a boundary-layer expansion in the glassy region (3.20).
$\dot{}$: used to indicate differentiation with respect to t (2.20) or τ (5.7).
$'$: used to indicate a dummy variable (2.1).
$[\cdot]_{\tilde{s}}$: jump across the front $\tilde{x}=\tilde{s}(\tilde{t})$, defined as $\cdot^{\mathrm{g}}(\tilde{s}^+(\tilde{t}),\tilde{t}) - \cdot^{\mathrm{r}}(\tilde{s}^-(\tilde{t}),\tilde{t})$.

References

[1] N. Thomas and A. H. Windle, A theory of case II diffusion, *Polymer* **23** (1982), 529–42.

[2] H. L. Frisch, Sorption and transport in glassy polymers—a review, *Polym. Eng. Sci.* **20** (1980), 2–13.

[3] C. J. Durning, D. A. Edwards and D. S. Cohen, Perturbation analysis of Thomas' and Windle's model of case II transport, *AIChE J.* **42** (1996), 2025–35.

[4] C. J. Durning and M. Tabor, Mutual diffusion in concentrated polymer solutions, *Macromolecules* **19** (1986), 2220–32.

[5] D. A. Edwards and D. S. Cohen, An unusual moving boundary condition arising in anomalous diffusion problems, *SIAM J. Appl. Math.* **55** (1995), 662–76.

[6] J. C. Wu and N. A. Peppas, Modeling of penetrant diffusion in glassy polymers with an integral sorption Deborah number, *J. Polym. Sci. B* **31** (1993), 1503–18.

[7] D. A. Edwards and D. S. Cohen, A mathematical model for a dissolving polymer, *AIChE J.* **41** (1995), 2345–55.

[8] T. P. Witelski, Traveling wave solutions for case II diffusion in polymers, *J. Polym. Sci. B* **34** (1996), 141–50.

[9] H. L. Frisch, T. K. Kwei and T. T. Wang, Diffusion in glassy polymers, II, *J. Polym. Sci. A-2* **7** (1969), 879–87.

[10] H. Fujita, Organic vapors above the glass transition temperature. *In Diffusion in Polymers*, J. Crank and G. S. Park, eds, Academic Press, New York 1968.

[11] L. H. Sperling, *Introduction to Physical Polymer Science*, 2nd ed. John Wiley and Sons, New York 1992.

[12] C. A. Kumins and T. K. Kwei, Free volume and other theories. *In Diffusion in Polymers*, J. Crank and G. S. Park, eds, Academic Press, New York 1968.

[13] R. G. Larson, *Constitutive Equations for Polymer Melts and Solutions.* Butterworths, Boston 1988.

[14] J. Crank and G. S. Park, Diffusion in high polymers: some anomalies and their significance, *Trans. Farad. Soc.* **47** (1951), 1072–84.

[15] H. C. Öttinger, *Stochastic Processes in Polymeric Fluids.* Springer-Verlag, New York 1996.

[16] J. Crank, A theoretical investigation of the influence of molecular relaxation and internal stress on the diffusion in polymers, *J. Polym. Sci.* **11** (1953), 151–68.

[17] D. S. Cohen, Theoretical models for diffusion in glassy polymers, *J. Polym. Sci. B* **21** (1983), 2057–65.

[18] D. S. Cohen, Theoretical models for diffusion in glassy polymers. II, *J. Polym. Sci. B* **22** (1984), 1001–09.

[19] N. F. Britton, Aggregation and the competitive exclusion principle, *J. Theor. Bio.* **136** (1989), 57–66.

[20] S. A. Gourley and N. F. Britton, Instability of travelling wave solutions of a population model with nonlocal effects, *IMA J. Appl. Math.* **51** (1993), 299–310.

[21] S. A. Gourley and N. F. Britton, A predator-prey reaction-diffusion system with nonlocal effects, *J. Math. Bio.* **34** (1996), 297–333.

[22] V. Alexaides and A. D. Soloman, *Mathematical Modeling of Melting and Freezing Processes.* Hemisphere, Washington 1993.

[23] C. E. Rogers, Solubility and diffusivity. *In Physics and Chemistry of the Organic Solid State*, vol. 2, D. Fox, M. M. Labes and A. Weissberger, eds, Wiley, New York 1965.

[24] D. A. Edwards, Constant front speed in weakly diffusive non-Fickian systems, *SIAM J. Appl. Math.* **55** (1995), 1039–58.

[25] D. S. Cohen and A. B. White, Jr., Sharp fronts due to diffusion and stress at the glass transition in polymers, *J. Polym. Sci. B* **27** (1989), 1731–47.

[26] C. K. Hayes and D. S. Cohen, The evolution of steep fronts in non-Fickian polymer-penetrant systems, *J. Polym. Sci. B* **30** (1992), 145–61.

[27] D. A. Edwards, Non-Fickian diffusion in thin polymer films, *J. Polym. Sci. B* **34** (1996), 981–97.
[28] C. Y. Hui, K. C. Wu, R. C. Lasky and E. J. Kramer, Case II diffusion in polymers. II. Steady state front motion, *J. Appl. Phys.* **61** (1987), 5137–49.
[29] B. A. Boley, A method of heat conduction analysis of melting and solidification problems, *J. Math. Phys.* **40** (1961), 300–13.
[30] D. A. Edwards, A mathematical model for trapping skinning in polymers, *Stud. Appl. Math.* **99** (1997), 49–80.
[31] C. J. Durning, Differential sorption in viscoelastic fluids, *J. Polym. Sci. B* **23** (1985), 1831–55.
[32] D. A. Edwards and D. S. Cohen, D. S., The effect of a changing diffusion coefficient in super-Case II polymer-penetrant systems, *IMA J. Appl. Math.* **55** (1995), 49–66.
[33] J. Crank, *The Mathematics of Diffusion*, 2nd ed. Oxford University Press, New York 1976.
[34] W. R. Vieth, *Diffusion in and Through Polymers: Principles and Applications.* Oxford University Press, New York 1991.
[35] J. E. Anderson and R. Ullman, Mathematical analysis of factors influencing the skin thickness of asymmetric reverse osmosis membranes, *J. Appl. Phys.* **44** (1973), 4303–11.

David A. Edwards
Department of Mathematical Sciences
University of Delaware
Newark, DE 19716-2553
USA
(e-mail: edwards@math.udel.edu)

(Received: June 22, 1999)